Title:	Dependency of punching shear resistance and membrane action on boundary conditions of reinforced concrete continuous slabs
Authors:	Belletti B., Ravasini S., Vecchi F., Muttoni A.
Published in:	6th International Symposium on Life-Cycle Civil Engineering (IALCCE)
Pages:	pp. 2745-2752
City, country:	Ghent, Belgium
Year of publication:	2019
Type of publication: EPFL InfoScience link:	Peer reviewed conference paper https://infoscience.epfl.ch/record/267717

Please quote as:	Belletti B., Ravasini S., Vecchi F., Muttoni A., *Dependency of punching shear resistance and membrane action on boundary conditions of reinforced concrete continuous slabs*, 6th International Symposium on Life-Cycle Civil Engineering (IALCCE), Ghent, Belgium, 2019, pp. 2745-2752.

Life-Cycle Analysis and Assessment in Civil Engineering: Towards an Integrated Vision – Caspeele, Taerwe & Frangopol (Eds)
© 2019 Taylor & Francis Group, London, ISBN 978-1-138-62633-1

Dependency of punching shear resistance and membrane action on boundary conditions of reinforced concrete continuous slabs

B. Belletti, S. Ravasini & F. Vecchi
Department of Engineering and Architecture, University of Parma, Parma, Italy

A. Muttoni
Ecole Polytechnique Fédérale de Lausanne, Lausanne, Switzerland

ABSTRACT The design of reinforced concrete flat slabs can be governed at failure by punching shear close to concentrated loads or columns. Geometrical features, reinforcement layouts and in-plane forces provided by external vertical elements, such as shear walls, can affect the membrane action and, consequently, the punching shear resistance. This paper presents a study on reinforced concrete continuous flat slab whose lateral expansion is restrained by the presence of vertical elements considering also shrinkage effects.

1 INTRODUCTION

It is widely recognized that Code formulations (Model Code 2010, Eurocode 2, ACI) are usually based on experimental tests carried out on isolated specimens. However, the actual behaviour of reinforced concrete slabs depends on moment redistribution, membrane action, geometrical parameters and other effects as the shrinkage strain of concrete.

Membrane action should be considered, together with moment redistribution, for the evaluation of punching shear resistance for concrete slabs, Figure 1a-b. These beneficial effects can be considered in the capacity assessment of actual slabs (Belletti et al. 2018), FRP members (Zeng et al. 2016), bridge deck slabs (Taylor et al. 2007, Kirkpatrick 2007), continuous RC and steel fibre reinforced slabs (Arshian et al. 2017, Amir et al. 2016, Foster et al. 2004, Ladner et al. 1977, Di Prisco et al. 2016), slabs subjected to fire (Bailey et al. 2001) or to a sudden removal of supporting columns (Dat et al. 2013, Gouverneur et al. 2013, Qian 2015).

Research devoted to these studies demonstrate the improvement of the bearing capacity of slabs provided by membrane actions. Membrane actions can be evaluated with FE method (Belletti et al. 2016), yield lines method (Bailey et al. 2001, Burgess et al. 2017), rigid-plastic approach (Wood 1961, Rankin 1997, Park 2000), axisymmetric assumptions (Einpaul et al. 2015, 2016). In the last years, membrane action was analysed using NLFEA and different modelling approach, for example using hexahedral elements (Genikomsou et al. 2017) or multi-layered shell elements (Belletti et al. 2016), where the latter provide good results with less computational cost.

This paper presents the results of a parametric investigation carried out to evaluate the dependency of membrane action and punching shear resistance on the reinforcement layout and boundary conditions. Indeed, vertical elements, such as shear walls or columns, can provide in-plane stiffness at boundaries. Nevertheless, also the case of fixed restrain on continuous slabs has been considered by preventing the horizontal displacement at boundaries in the first load case, when dead load of slab and shrinkage of concrete have been applied, or in the second load case when the distributed load is applied to the slab. Therefore, in this paper, the

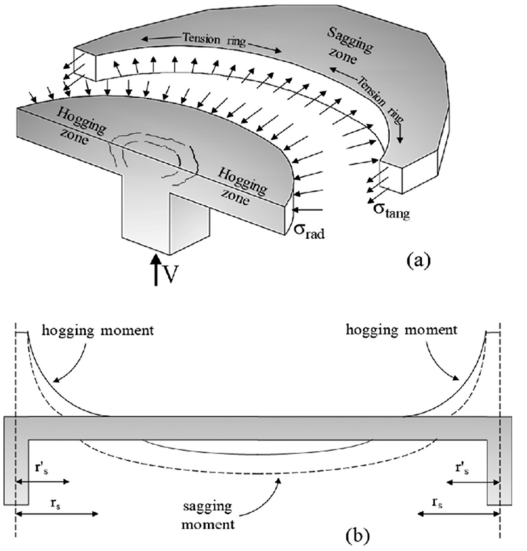

Figure 1. (a) Membrane Action – radial and tangential stresses (σ_{rad} and σ_{tang}) and effect of the tension ring on the hogging area; (b) Moment redistribution between hogging and sagging areas.

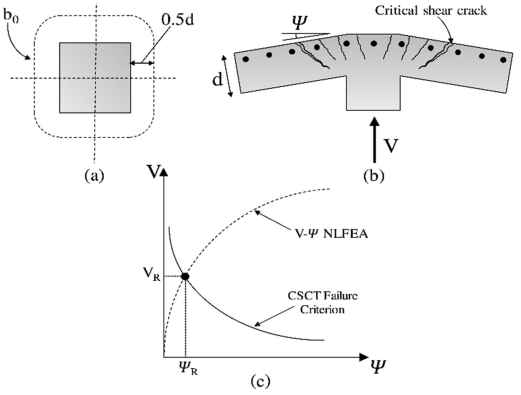

Figure 2. (a) Assumption of control perimeter at 0.5*d* from the edge of the column; (b) Punching shear strength correlated to the crack opening; (c) Punching shear resistance at the intersection between non-linear load-rotation curve and CSCT failure criterion.

effects of these different boundary conditions, different ratios of hogging and sagging reinforcement and shrinkage effect have been considered.

Nonlinear finite element analyses (NLFEA) are performed using a multi – layered shell model and PARC_CL 2.0 crack model (Belletti et al. 2017) implemented as user subroutine in Abaqus Code. Numerical results are then post–processed adopting the Critical Shear Crack Theory (CSCT) (Muttoni et al. 2008).

In the framework of the Level of Approximation (LoA) approach, comparisons of the punching shear resistance evaluated with and without considering moment redistribution, membrane action and shrinkage effects, have been carried out.

2 CSCT FAILURE CRITERION AND PARC_CL 2.0 CRACK MODEL

The CSCT failure criterion is able to predict the punching shear resistance of a slab, subjected to a concentrated load, as function of the maximum slab rotation Ψ, Figure 2b. The formula for the failure criterion (Muttoni 2008, Guidotti 2010, Muttoni et al. 2017) is given in Eq. (1):

$$V_{R(\psi)} = \frac{\frac{3}{4} b_0 d \sqrt{f_c}}{1 + 15 \frac{\psi d}{d_g + d_{g0}}} \quad (1)$$

where b_0 is the length of the control perimeter at distance 0.5*d* from the column edge, Figure 2a, *d* is the effective depth of the slab, f_c is the concrete compressive strength in [MPa], d_g is the maximum aggregate size, and d_{g0} is the reference aggregate size (16 mm). Punching shear failure occurs at the intersection between the load-rotation curve (obtained from NLFEA) and the CSCT failure criterion, Figure 2c.

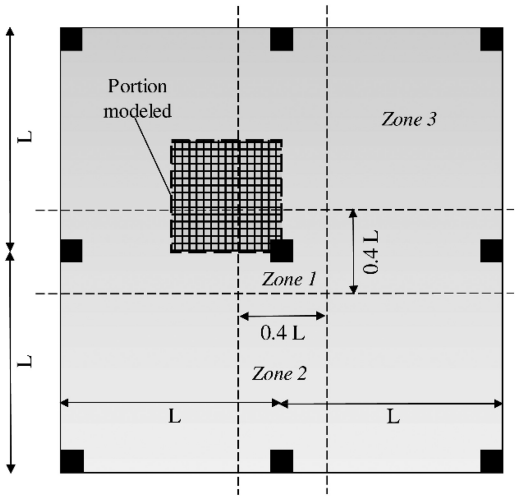

Figure 3. Self confined slab: portion of modelled slab and layout of reinforcements zones.

Table 1. Mechanical properties of steel and concrete.

f_c [MPa]	f_y [MPa]	E_c [MPa]	E_s [MPa]
35	520	32600	200000

Nonlinear Finite Element Analyses (NLFEA) are performed using multi – layered shell elements approach and PARC_CL 2.0 (Belletti et al. 2017) crack model which is implemented as user subroutine in Abaqus Code and it is able to account for hysteretic loops and plastic deformations under cyclic loading. Mechanical nonlinearity of concrete and steel, aggregate interlock and multiaxial state of stress for concrete are considered. To evaluate membrane actions, the geometric nonlinearity has been considered adopting a Lagrangian formulation.

Since multi-layered shell elements are not able to predict the nonlinear behaviour over the thickness of the slab, a post-processing based on the Critical Shear Crack Theory (Muttoni 2008) is applied.

3 SHRINKAGE, MEMBRANE ACTION AND MOMENT REDISTRIBUTION EFFECTS ON PUNCHING SHEAR RESISTANCE

3.1 *Case study*

In this paper, a case study extracted from a parametric analysis carried out in Belletti et al. (2018) has been selected to investigate the dependency of the punching resistance of RC continuous slabs on stiffening effects of boundary conditions.

The mechanical properties for concrete and steel are indicated in Table 1; while the geometrical parameters of the slabs (column size *c*, thickness *h*, effective depth *d*, span between adjacent columns *L*) are reported in

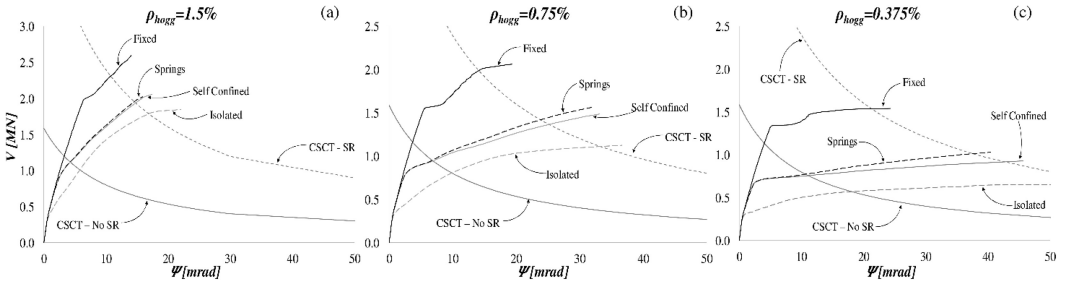

Figure 4. Load-rotation curves vs CSCT failure criterion without shrinkage effect for: (a) $\rho_{hogg} = 1.5\%$, (b) $\rho_{hogg} = 0.75\%$, (c) $\rho_{hogg} = 0.375\%$.

Table 2. Geometrical parameters for the analyses.

c [mm]	L [m]	h [mm]	d [mm]
260	6	250	210

Table 2. Three cases with three different hogging reinforcement ratios in the column area (0.4 L x 0.4 L) are studied: ρ_{hogg} *= 1.5%, 0.75%, 0.375%.* The sagging reinforcement is uniformly distributed over the span with a reinforcement ratio ρ_{sagg} / ρ_{hogg} equal to 1/3 in *Zone 1*, to 2/3 in *Zone 2* and to 1 *Zone 3*, as indicated in Figure 3c.

Since membrane actions are strongly dependent on slab boundary conditions, different cases are investigated (Figure 3):

– *Isolated slab* reproducing the hogging area of a flat slab having dimensions *0.22L x 0.22L* corresponding to experimental test set-up;
– *Self-confined continuous flat slab* with regular spans *L* loaded with a uniform pressure, simulating permanent and variable loads (Figure 3);
– *Continuous flat slab restrained with horizontal stiffening springs* having regular spans *L* loaded with a uniform pressure. Non-linear springs having no-tension behaviour and compressive stiffness, calculated assuming as vertical members RC wall 3.50 m high and 0.3 m thick, have been used;
– *Fully restrained continuous flat slab* with regular spans *L* loaded with a uniform pressure, which lateral displacements set equal to zero.

Since shrinkage may affect the crack pattern in different way depending on the erection phases of buildings, this last case is divided into two subcases:

1. *Fixed restrained continuous slab*: the lateral displacements at boundaries are restrained before the application of shrinkage, self-weight and pressure load;
2. *Post-Fixed restrained continuous slab*: the lateral displacements at boundaries are restrained after the application of shrinkage and self-weight but before the application of pressure load.

In both cases, membrane action effect is considerable if compared to isolated specimens. Shrinkage effect, in unsaturated environment, causes an anticipate cracking of concrete specimens, leading to a decrease of bearing capacity. This problem becomes more serious if slab contraction is restrained. A constant shrinkage strain ε_{sh} equal to $3 \cdot 10^{-4}$ is considered, as an additional tensile strain in PARC_CL2.0 crack model (Belletti et al. 2018).

3.2 *Punching shear resistance*

In Figure 4, the load-rotation curves without shrinkage effect for isolated specimen, self-confined continuous flat slab and laterally restrained slabs with springs and fixed boundary conditions are shown. To appreciate the difference between the resistance of flat slabs without and with shear reinforcement (SR), the failure criterion associated to shear reinforcement is also considered.

In case of lateral stiffening provided by shear walls, (the so called *"Spring"* case), the increasing of punching shear resistance with respect to the self-confined slab is very limited and the resistance increases as the hogging reinforcement decreases. There are no differences for the *"Fixed"* and *"Post-Fixed"* cases because the shrinkage effect is not considered.

Figure 5 shows the influence of concrete shrinkage on the punching shear resistance for all the cases investigated. Shrinkage effects on punching shear resistance are more evident in the *"Fixed"* case, causing anticipated cracking of the slab and initial loss of stiffness. For *"Post-Fixed"* case initial loss of stiffness is not observed because the shrinkage is imposed before lateral displacement restraining. *"Springs"* and *"Self-Confined"* resistances with shrinkage effects are lower than without shrinkage effects. The shrinkage effect for *"Isolated"* cases is quite negligible.

3.3 *Membrane action effect*

The dilatation of cracked concrete in the hogging area is restrained by the outer part of the slab, leading to the formation of radial and tangential stresses, respectively σ_{rad} and σ_{tang}.

This phenomenon increases stiffness and consequently the strength of slabs (Einpaul 2015 et al., Einpaul 2016 et al., Belletti et al. 2013, 2015). The

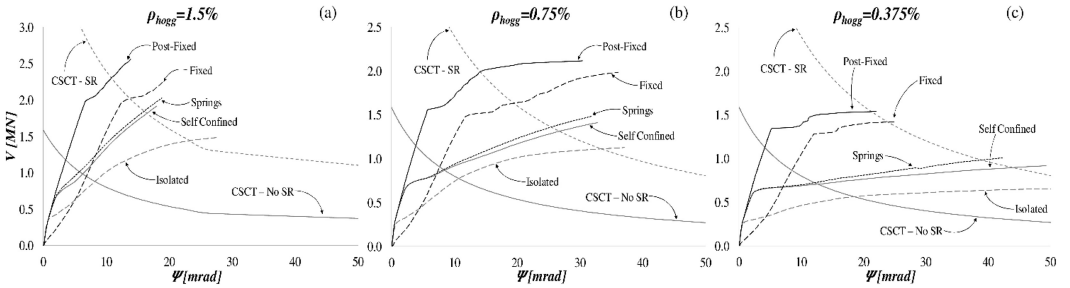

Figure 5. Load-rotation curves vs CSCT failure criterion with shrinkage effect for: (a) $\rho_{hogg} = 1.5\%$, (b) $\rho_{hogg} = 0.75\%$, (c) $\rho_{hogg} = 0.375\%$.

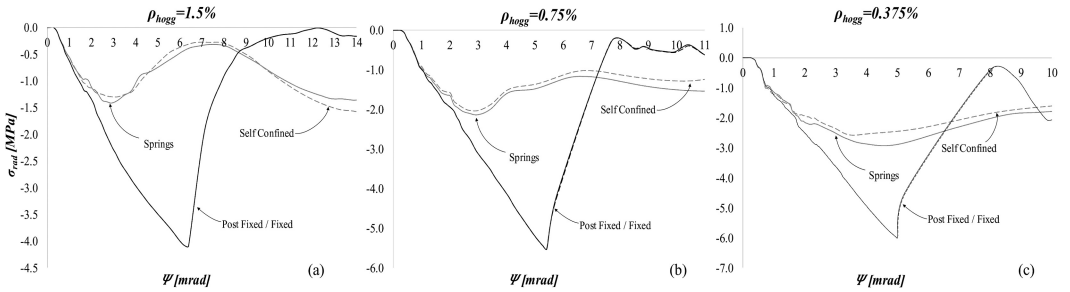

Figure 6. Radial stress without shrinkage effect for: (a) $\rho_{hogg} = 1.5\%$, (b) $\rho_{hogg} = 0.75\%$, (c) $\rho_{hogg} = 0.375\%$.

average values of radial stresses σ_{rad}, over the control perimeter b_0 at distance $0.5d$ from the edge of the column, have been calculated using NLFEA on continuous slabs.

Figure 6 shows the graph radial membrane action σ_{rad} vs slab rotation for the cases without shrinkage effect. For *"Springs"* case a negligible increment of σ_{rad} is observed, as expected. No differences between the *"Fixed"* and *"Post-Fixed"* cases can be obtained without shrinkage effects.

Figure 7a-c shows the radial membrane action σ_{rad} vs slab rotation for the cases with shrinkage effect. As expected, the concrete shrinkage leads to a reduction of radial stress σ_{rad}.

For *"Fixed"* case, due to the anticipated cracking of continuous slab, an initial tensile radial stress can be registered in the graph σ_{rad} vs Ψ, causing a reduction of the compressive radial stress σ_{rad} peak and, consequently, a reduction of the punching shear resistance. For *"Springs"* case, applied before the application of shrinkage effects and self-weight, Figure 7a-c shows a similar trend than "*Fixed"* case but with lower consequences. For *"Post-Fixed"* case, the confining effects, achieved with fixed restrain of lateral displacement, can provide the maximum values of radial stresses. Figure 7d reports the values of initial tensile stress and the peak values of compressive radial stress as a function of the hogging reinforcement ratio over the column. As expected, the maximum tensile stresses, causing anticipated cracking, is occurring for highest reinforcement ratios; at the contrary the maximum compressive radial stresses can be encountered for lowest reinforcement ratios.

Higher compressive stresses are observed in case of lower reinforcement ratios due to the higher difference between the stiffness in hogging and sagging zones.

Figure 5 and Figure 7 demonstrate that, for brittle failure mode (like shear and shear punching failure mode), the shrinkage effects at early stage and boundary conditions (connected to the erection phases of buildings) can severely affect the serviceability and ultimate limit states. Furthermore, Figure 5 and Figure 7 show that membrane actions and punching shear resistance are affected by shrinkage effects in different measure depending not only on boundary conditions but also on reinforcement ratios.

Figure 8 shows radial stress σ_{rad} for the *"Post-Fixed"* and *"Fixed"* cases considering shrinkage of concrete. The most interesting "events" are marked on radial membrane action σ_{rad} vs slab rotation Ψ: cracking of concrete (corresponding to ε_{cr}), maximum crack opening (corresponding to w_{ctu}, calculated as $w_{ctu} = \varepsilon_{ctu} \cdot a_m$ where am is the distance between cracks, see Belletti et al. 2017), yielding strain of hogging and sagging reinforcement (ε_{sy}). It can be noted from Figure 8a-c, that the peak value of radial stresses σ_{rad} occurs when the maximum crack opening w_{ctu} (corresponding to a zero residual tensile stress) is achieved in the sagging area, since this circumstance corresponds to the maximum tension ring effect. Depending on the intersection between NLFEA curve and CSCT failure criterion, punching shear failure occurs before yielding of hogging reinforcement for high reinforcement ratio ($\rho_{hogg} = 1.5\%$), after yielding of hogging reinforcement but before yielding of sagging reinforcement for medium and low reinforcement ratio

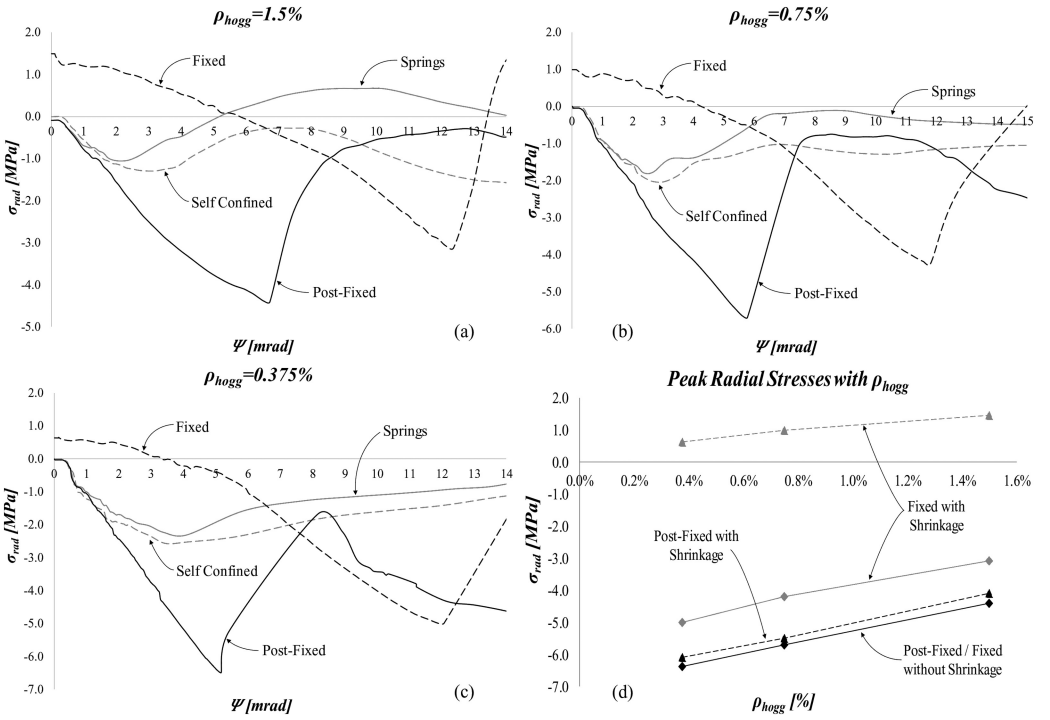

Figure 7. Radial stress with shrinkage effect for: (a) $\rho_{hogg} = 1.5\%$, (b) $\rho_{hogg} = 0.75\%$, (c) $\rho_{hogg} = 0.375\%$, (d) Peak tensile and compressive stresses with ρ_{hogg}.

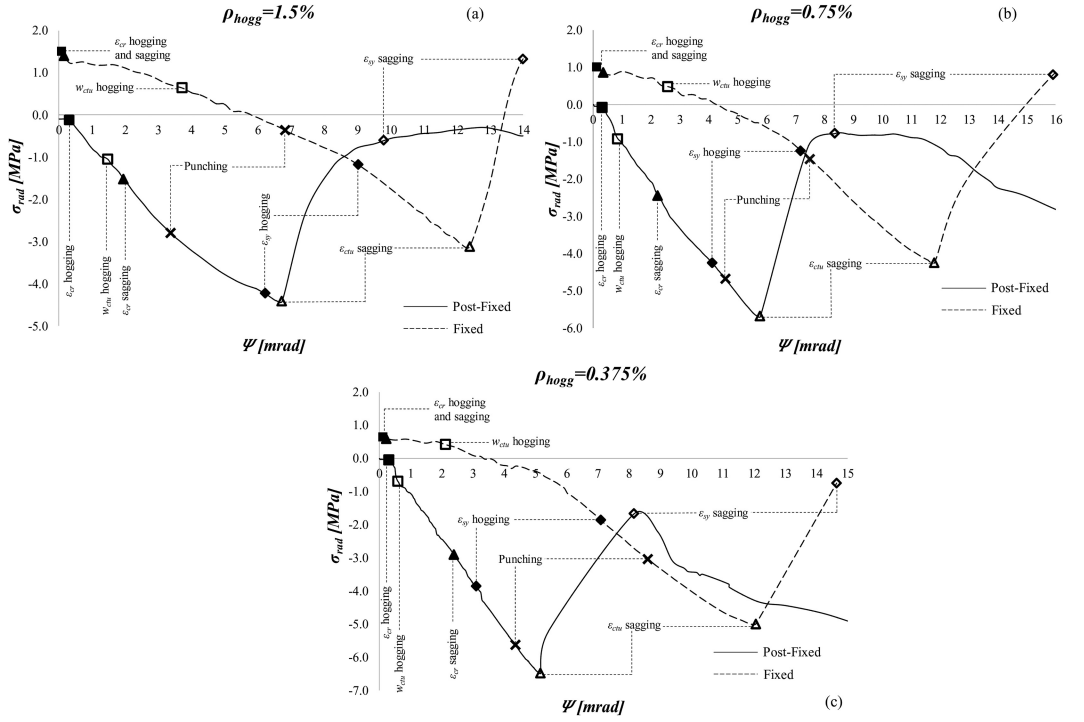

Figure 8. Radial stress with shrinkage effect for "Fixed" and "Post-Fixed" cases: (a) $\rho_{hogg} = 1.5\%$, (b) $\rho_{hogg} = 0.75\%$, (c) $\rho_{hogg} = 0.375\%$.

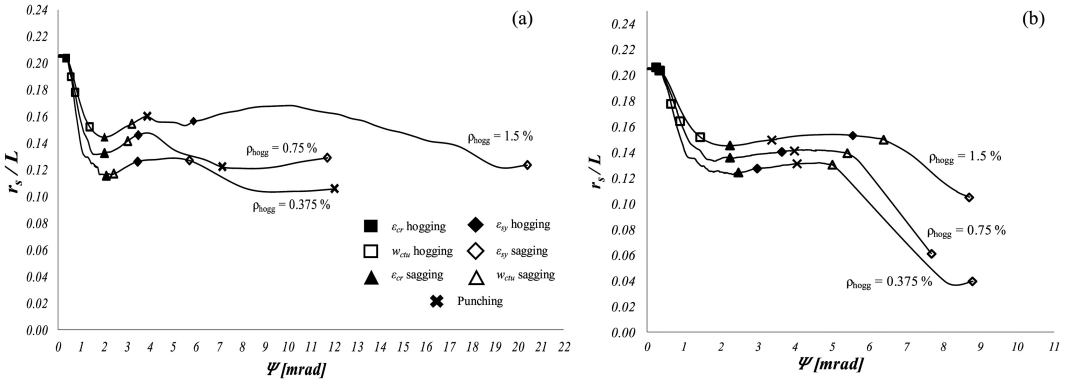

Figure 9. Variation of the point of contraflexure rs as function of the rotation Ψ without shrinkage effect: (a) "*Self − Condined*" slab, (b) "*Post − Fixed*" (or "*Fixed*") case.

(ρ_{hogg} = *0.75%* and ρ_{hogg} = *0.375%*). Note that for the *"Fixed"* case, the cracking of hogging and sagging zone are almost simultaneous because of tensile in-plane stresses. The achievement of w_{ctu} corresponds to the first plateau observed in load-rotation curves Figure 4 and 5.

It is important to observe that the sequence of aforesaid events is the same also without considering shrinkage effect.

3.4 *Moment redistribution effect*

The most significant assumption of design methods consists in a constant position of the contraflexure point at 0.22*L*, that is valid for isolated elements up to failure. However, for self-confined or fully confined slabs, moment redistribution occurs after the loss of stiffness in the hogging area due to cracking of concrete, triggering to a reduction of r_s.

Figure 9 shows the variation of the point of contraflexure r_s with the slab rotation Ψ, neglecting the shrinkage effect. Before cracking in the hogging area, the position of this point remains constant and corresponds approximately to 0.22*L*, as expected, then it tends to move closer to the column. Figure 9a shows the position of the point of contraflexure r_s for a *"Self-Confined"* slab; Figure 9b shows the *"Post-Fixed"* case (equivalent of *"Fixed"* case if shrinkage effect is neglected), where r_s tends to decrease more than for self-confined slab, leading to an increment of the punching shear resistance. After a rotation Ψ about *2 mrad*, the point of contraflexure tends to move again to the column, for both cases. It is important to point out that the changing position of r_s is more pronounced for low reinforcement.

4 ASSESSMENT OF PUNCHING SHEAR RESISTANCE BY USING LEVELS OF APPROXIMATION

LoA IV, achieved using NLFEA, provides the highest punching shear capacities. Membrane action and moment redistributions can be accounted for in analytical calculations using an iterative procedure and adopting LoA II and LoA III.The slab rotation Ψ proposed by fib-Model Code 2010 for LoA II is, Eq. (2):

$$\psi = 1.5\frac{r_s}{d}\frac{f_y}{E_s}\left(\frac{m_E}{m_R}\right)^{1.5} \tag{2}$$

where r_s is the distance between the column axis and the point of contraflexure, f_y is the yield strength of the reinforcement steel, E_s is the steel modulus of elasticity, m_E is the average moment per unit length of the flexural reinforcement in hogging area and m_R is the average flexural resistance of the slab in the hogging area.

For LoA I, it is assumed that the flexural reinforcement in the hogging area is fully plasticized, so rotation Ψ may be calculated assuming $m_E/m_R = 1$.

For the LoA II, m_E is estimated on the basis of the acting shear force V_E ($m_E = V_E/8$for an interior symmetric column). An iterative procedure is adopted until $V_E = V_R$ for calculating the punching shear resistance. In the LoA III, linear finite element analyses (LFEA) can be used to estimate m_E and r_s. For LoA IV, the load-rotation relationship is replaced by a relationship determined using non-linear finite element analysis (NLFEA).

In this paper is presented a procedure to calculate analytically the punching shear resistance using LoA II and LoA III by accounting for both membrane action and moment redistribution, on the basis of σ_{rad} vs Ψ and r_s vs Ψ graphs pre-elaborated from NLFEA results. This iterative approach can be summarized in the flow-chart in Figure 10.

The separated effect of membrane action or moment redistribution are also considered, to appreciate the impact of each contribution on the punching shear resistance assessment. Therefore, in Figure 11 the normalized punching shear resistance, obtained using LoA IV, which refers to NLFEA results, is compared to the resistances obtained with the analytical procedure using LoA II and LoA III, Figure 10.

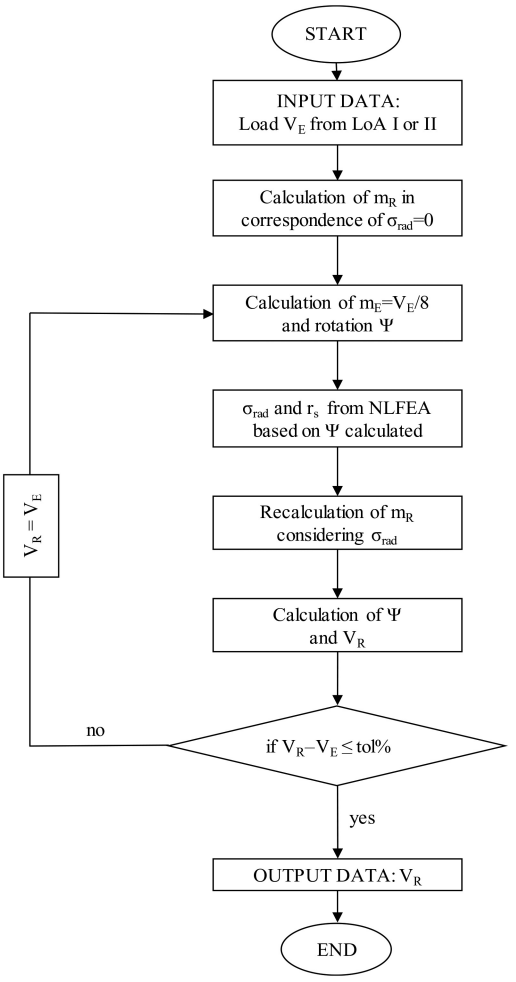

Figure 10. Flow-chart for iterative calculation of punching shear resistance for LoA II and III.

In Figure 11, normalized punching shear resistances, obtained using LoA II and LoA III, are calculated according to the hypotheses reported in Table 3.

Analytical calculations of the punching shear resistance of continuous flat slabs for LoA II and LoA III is improved if membrane action and moment redistribution are considered.

For case (d), the punching shear resistance results lower compared to other cases due to anticipated cracking caused by tensile radial stresses.

It is worth to remark that the analytical procedure presented in this paper represents a refinement of Model Code 2010 (fib, 2013) formulations able to account, during the iterative procedure, for membrane action and moment redistribution expressed as function of slab rotation. The presented procedure leads to punching shear resistances close to the values obtained using LoA IV.

Table 3. Assumptions for improved calculations according to LoA II and III.

	Membrane action	Moment redistribution
Case (a)	accounted for by calculating m_R on the basis of the radial stresses σ_{rad} – *"Self-confined"* constraints without shrinkage – Figure 7	accounted for by calculating r_s – *"Self-confined"* constraints without shrinkage – Figure 10
Case (b)	accounted for by calculating m_R on the basis of the radial stresses σ_{rad} – *"Springs"* constraints without shrinkage – Figure 7	Neglected (fixed value of r_s)
Case (c)	accounted for by calculating m_R on the basis of the radial stresses σ_{rad} – *"Post-Fixed"* constraints without shrinkage – Figure 7	accounted for by calculating r_s – *"Post-Fixed"* constraints without shrinkage – Figure 10
Case (d)	accounted for by calculating m_R on the basis of the radial stresses σ_{rad} – Case of *"Fixed"* constraints with shrinkage – Figure 8	Neglected (fixed value of r_s)

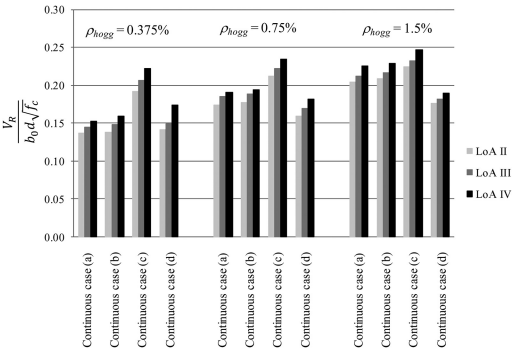

Figure 11. Comparison of the normalized punching shear resistance of case (a), (b), (c) and (d) where the LoA II and III are improved accounting for moment redistribution and membrane action effect and LoA IV corresponds to NLFEA.

5 CONCLUSIONS

This paper presents the results of a study that aims to evaluate the dependency of the punching shear resistance on moment redistribution and membrane action effects. These latter effects have been investigated considering their dependency on boundary conditions and shrinkage of concrete.

The main conclusions are:

– The punching shear resistance of laterally restrained slabs is higher than the one of self-confined slabs. The entity of lateral constraints is strongly correlated to the boundary conditions and stiffness provided by vertical elements.
– Shrinkage of concrete leads to a reduction of membrane action and, consequently, of punching shear resistance. This effect is more pronounced for slabs with high reinforcement ratios (where restrained deformations cause higher tensile membrane stresses with anticipated cracking). Therefore, shrinkage effect is also strongly depending on boundary conditions and erection phases of buildings.
– In the framework of Level of Approximation approach, a refinement of the Model Code 2010 (fib, 2013) formulation, for the assessment of punching shear resistance according to LoA II and III, has been presented. The iterative procedure is able to account for membrane action and moment

redistribution, leading to a better estimation of the punching shear resistance of continuous slabs.
– The LoA IV, achieved using NLFEA, remains the most refined level to evaluate the bearing capacity of reinforced concrete slabs. NLFEA results could be also used to formulate expression for membrane action or moment redistribution to be adopted to refine analytical calculations.

REFERENCES

ACI Comittee 318, 2014. Building Code Requirements for Structural Concrete (ACI 318-14) and Commentary.

Amir, S., Van Der Veen, C., Walraven, J.C., De Boer, A. 2016. Experiments on punching shear behavior of prestressed concrete bridge decks. ACI Structural Journal 113(3), pp. 627–636.

Arshian A. H., Morgenthal G. 2017. Probabilistic assessment of the ultimate load-bearing capacity in laterally restrained two-way reinforced concrete slabs. Engineering Structures 150 52–63.

Bailey CG. Membrane action of unrestrained lightly reinforced concrete slabs at large displacements. Eng Struct 2001; 23:470–83.

Belletti, B., Walraven, J.C., Trapani, F. (2015) Evaluation of compressive membrane action effects on punching shear resistance of reinforced concrete slabs. Engineering Structures, 95(7): 25–39.

Belletti, B., Pimentel M., Scolari M., Walraven, J.C. (2015). Safety assessment of punching shear failure according to level of approximation approach. Structural Concrete, 16(3): 366–380.

Belletti B., Damoni C., Cervenka V., Hendriks M.A.N. (2016). Catenary action effects on the structural robustness assessment of RC slab strips subjected to shear and tensile forces. Structural Concrete Volume 17, Issue 6, 1 December 2016, Pages 1003–1016.

Belletti, B., Scolari, M., Vecchi, F. 2017. PARC_CL 2.0 crack model for NLFEA of reinforced concrete structures under cyclic loadings. Computers and Structures 191, pp. 165–179.

Belletti, B., Muttoni, A., Ravasini, S., Vecchi, F. 2018. Parametric analysis on punching shear resistance of reinforced concrete continuous slabs. Engineering Structures, under submission.

Bernardi P., Cerioni R., Michelini E., Sirico A. (2016). Numerical simulation of early-age shrinkage effects on RC member deflections and cracking development. Frattura ed Integrità Strutturale. 10, 15–21. 10.3221/IGF-ESIS.37.03.

Botte W. 2017 Quantification of Structural Reliability and Robustness of New and Existing Concrete Structures Considering Membrane Action. PhD thesis, Ghent University.

Burgess I. 2017. Yield-line plasticity and tensile membrane action in lightly-reinforced rectangular concrete slabs. Engineering Structures 138. 195–214.

Cantone, R., Belletti, B., Manelli, L., Muttoni, A. 2016. Compressive membrane action effects on punching strength of flat RC slabs. Key Engineering Materials 711, pp. 698–705.

Clément T., Pinho Ramos A. Fernández Ruiz M., Muttoni A. 2014 Influence of prestressing on the punching strength of post-tensioned slabs. Engineering Structures 72: 56–69.

Dat PX, Hai TK. 2013. Membrane action of RC slabs in mitigating progressive collapse of building structures. Eng Struct 2013; 55:107–15.

Di Prisco, M., Martinelli, P., Parmentier, B. 2016. On the reliability of the design approach for FRC structures according to fib Model Code 2010: the case of elevated slabs. Structural Concrete 17 (4), pp. 588–602.

Einpaul J., Ruiz M. F., Muttoni A. (2015). Influence of moment redistribution and compressive membrane action on punching strength of flat slabs. Engineering Structures 86: 43–57.

Einpaul J., Ospina C.E., Ruiz M.F., Muttoni A. (2016). Punching Shear Capacity of Continuous Slabs. ACI Structural Journal, 113(4), pp. 861–872.

Eurocode 2. Design of Concrete Structures—General Rules and Rules for Buildings, EN 1992-1-1. Brussels, Belgium: CEN European Committee for Standardization; 2004; 225 p.

Fib – International federation for structural concrete. fib model code for concrete structures 2010. Ernst & Sohn; 2013; 434 p.

Foster S.J., Bailey C.G., Burgess I.W. & Plank R.J. (2004) Experimental behaviour of concrete floor slabs at large displacements. Engineering Structures 26(9):1231–47.

Genikomsou A. S., Polak M. A. 2017. 3D finite element investigation of the compressive membrane action effect in reinforced concrete flat slabs. Engineering Structures 136. 233–244.

Gouverneur D., Caspeele R. & Taerwe L. (2013a) Experimental investigation of the load-displacement behaviour under catenary action in a restrained reinforced concrete slab strip. Engineering structures 49: 1007–1016.

Guidotti R. Poinçonnement des planchers-dalles avec colonnes superposées fortement sollicitées (Doctoral thesis, in French), 2010; EPFL, Lausanne, Switzerland, p. 230.

Kirkpatrick J, Rankin G, Long A. The influence of compressive membrane action on the serviceability of beam and slab bridge decks. Struct Eng 1986; 64B(1): 6–12.

Ladner M, Schaeidt W, Gut S, 1977. Experimentelle Untersuchungen an Stahlbeton-Flachdecke. EMPA Bericht no. 205, Switzerland. 96p. [in German].

Muttoni A., 2008. Punching shear strength of reinforced concrete slabs without transverse reinforcement. ACI Structural Journal, 105 440–50.

Muttoni A, Fernández Ruiz M, Simões JT. 2017. The theoretical principles of the critical shear crack theory for punching shear failures and derivation of consistent closed-form design expressions. Structural Concrete: 1–17.

Park, R., Gamble, W.L., Reinforced Concrete Slabs, second ed., John Wiley, New York, USA, 2000, p. 736.

Qian, K., Li, B., Zhang, Z. 2015. Testing and simulation of 3D effects on progressive collapse resistance of RC buildings. Magazine of Concrete Research, 67(4), pp. 163–178.

Rankin, G.I.B., Long, A.E., Arching action strength enhancement in laterally restrained slab strips, Proc. ICE Struct. Build. 122 (4) (1997) 461–467.

Shu J., Belletti B., Muttoni A., Scolari M., Plos M. 2017. Internal force distribution in RC slabs subjected to punching shear. Engineering Structures 153: 766–781.

Taylor SE, Rankin B, Cleland DJ, Kirkpatrick J. Serviceability of bridge deck slabs with arching action. ACI Struct J 2007;104(1):39–48.

Wood R.H. (1961) Plastic and elastic design of slabs and plates, with particular reference to reinforced concrete floor slabs. London: Thames and Hudson.

Zeng Y, Caspeele R., Matthys S., Taerwe L. 2016. Compressive membrane action in FRP strengthened RC members. Construction and Building Materials 126: 442–452.